Research Square

Preprints are preliminary reports that have not undergone peer review.
They should not be considered conclusive, used to inform clinical practice,
or referenced by the media as validated information.

Antimicrobial activity of açaí (Euterpe oleracea Mart.) seed pyrolysis bio-oil against methicillin-resistant Staphylococcus aureus: in vitro assays and a wounded human organotypic skin explant (hOSEC) model

Lara Fabian Teixeira Lisboa
Universidade de São Paulo
Camila Veiga De Souza Gonçalves
Universidade Federal do Pará
Lauro Henrique Hamoy Guerreiro
Universidade Federal do Pará
Pedro Soler Coltro
Universidade de São Paulo
Endrigo Piva Pontelli
Lotus Clinic
Nélio Teixeira Machado
Universidade Federal do Pará
Marco Andrey Cipriani Frade
Universidade de São Paulo
Filipe Rocha Lima
filipelima@usp.br
Universidade de São Paulo
Marta Chagas Monteiro
Universidade Federal do Pará

Research Article

Keywords: Euterpe oleracea, pyrolysis bio-oil, human skin explant, antimicrobial activity

Posted Date: November 20th, 2026

DOI: https://doi.org/10.21203/rs.3.rs-11639292/v1

License: This work is licensed under a Creative Commons Attribution 4.0 International License.
Read Full License

Additional Declarations: No competing interests reported.

Abstract

Methicillin-resistant *Staphylococcus aureus* (MRSA) causes skin and soft-tissue infections, and new topical agents are needed. Açaí (*Euterpe oleracea* Mart.) seeds are an Amazonian agro-industrial residue whose pyrolysis bio-oil is rich in phenolic compounds. This study evaluated açaí bio-oil against *S. aureus in vitro* and in the human organotypic skin explant culture model (hOSEC). Bio-oils were obtained by pyrolysis of 1 M NaOH-impregnated açaí seeds at 350, 400, and 450°C and characterised for acid value, density, and viscosity. Cytotoxicity was assessed by MTT assay in NIH-3T3 fibroblasts and HaCaT keratinocytes; minimum inhibitory and bactericidal concentrations (MIC/MBC) against MRSA NCTC 12493 by resazurin microdilution; reactive oxygen species (ROS) by H2DCFH-DA fluorescence; tissue tolerability by TTC assay in hOSEC; and topical antibacterial activity in wounded hOSEC colonised with *S. aureus* ATCC BAA-1026. MIC and MBC were 1000 µg/mL for the 350°C bio-oil and 500 µg/mL for the 400 and 450°C bio-oils, indicating weak-to-moderate bactericidal activity. Monolayer CC_{50} values (115.5–305.3 µg/mL) were below the MICs (selectivity index 0.13–0.37), whereas skin explants showed greater tolerance (CC_{50} > 1000 µg/mL; viability ≥ 53% at 1000 µg/mL after 120 h). In wounded hOSEC, the 350°C and 450°C bio-oils at 1000 µg/mL reduced *S. aureus* counts to near the detection limit at 24 h, outperforming the antibiotic–antimycotic control ($p = 0.0483$ and $p = 0.0446$). Açaí seed bio-oil exhibits bactericidal activity against MRSA and is tolerated by skin tissue at effective concentrations, supporting its potential as a topical antimicrobial.

1. Introduction

Antimicrobial resistance (AMR) is one of the main threats to global health; in 2019, bacterial AMR was directly responsible for an estimated 1.27 million deaths worldwide, and methicillin-resistant *Staphylococcus aureus* (MRSA) was among the pathogen–drug combinations with the highest attributable burden (Murray et al. 2022). A major contributing factor is the indiscriminate use of antibiotics in clinical practice (Ceará 2021), which increases the risk of bacterial resistance (FIOCRUZ 2024). *S. aureus* is a Gram-positive coccus and the leading cause of skin and soft-tissue infections, ranging from impetigo and furunculosis to infected wounds and ulcers that can progress to invasive disease (Costa et al. 2024). Its pathogenicity relies on a broad arsenal of adhesins, toxins and immune-evasion factors that enable invasion of the different skin layers (Cheung et al. 2021). As resistance to first-line and topical agents spreads, treatment options narrow and new antimicrobial candidates are needed (Shaaban et al. 2024).

Natural products remain a major source of antimicrobial scaffolds. Brazil is the world's leading producer, consumer and exporter of açaí (*Euterpe oleracea* Mart.), and the processing of the fruit generates large amounts of seeds that are discarded as waste (Feitoza et al. 2022; Nobre et al. 2023). Açaí oil and pulp have documented biological activities, including antioxidant and anti-inflammatory effects (Magalhães et al. 2021), use in nanoemulsions for photodynamic therapy (Monge-Fuentes et al. 2017) and inhibition of *S. aureus* biofilm formation (Dias-Souza et al. 2018). The seeds, in turn, are a lignocellulosic biomass that can be converted by pyrolysis into bio-oil, a complex liquid containing hydrocarbons and an

oxygenated fraction rich in phenols (Sousa et al. 2021; Valdez et al. 2023). Chemical activation of the seeds with alkali (NaOH) before pyrolysis improves bio-oil yield, hydrocarbon content and antioxidant capacity (Valdez et al. 2023; Valois et al. 2024). Preliminary data indicate that açaí seed bio-oil has antimicrobial activity that depends on pyrolysis temperature (Silva et al. 2024a), but its activity against MRSA and its safety for human skin have not been investigated.

Assessing topical antimicrobials requires models that reproduce the barrier function and cellular complexity of human skin. Monolayer cultures lack the stratum corneum and the extracellular matrix and therefore tend to overestimate toxicity, while animal skin differs from human skin in thickness, hair density and immune composition. The human organotypic skin explant culture (hOSEC) preserves the native architecture of human skin, including keratinocytes, melanocytes, Langerhans cells, dermal fibroblasts, appendages and the dermo-epidermal junction, and remains viable in culture for up to 60–75 days (Frade et al. 2015; Leite 2021a). The model has been used to study the cutaneous distribution of dacarbazine (Leite et al. 2021b) and ibrutinib (Souto-Silva et al. 2024), to maintain *Mycobacterium leprae* for up to 60 days (De Paula et al. 2024), and, more recently, to establish an epidermal *S. aureus* colonisation model (Lisboa et al. 2026). Such human-relevant new approach methodologies (NAMs) are now encouraged by regulatory agencies as alternatives to animal testing in drug development, in line with the 3Rs principle (Pedro 2021; Avelino et al. 2024; De Barros et al. 2025; Da Silva et al. 2026; FDA 2026; Wu et al. 2026).

We hypothesised that (I) pyrolysis temperature modulates the antibacterial activity of açaí seed bio-oil and (II) human skin tissue tolerates bio-oil concentrations that are cytotoxic to monolayer cells, allowing topical antibacterial activity without tissue damage. To test these hypotheses, we produced bio-oils from NaOH-impregnated açaí seeds at 350, 400 and 450°C and evaluated their physicochemical properties, cytotoxicity in skin cell lines, bactericidal activity against MRSA, effect on bacterial ROS, tolerability in hOSEC and antibacterial efficacy in a wounded hOSEC infection model. To our knowledge, this is the first study to evaluate a pyrolysis bio-oil as a topical antimicrobial in an ex vivo human skin infection model. Given the foregoing, this study aimed to evaluate the antimicrobial potential of açaí (*E. oleracea*) bio-oil against *S. aureus in vitro* and in an hOSEC model.

2. Materials and methods

2.1. Production of açaí seed bio-oil

Açaí (*E. oleracea*) seeds were collected from açaí processing establishments in the Guamá neighbourhood of Belém, Pará, Brazil (1°28'04" S, 48°27'30" W). A batch of 750 kg of seeds was dried at 110°C for 24 h in a forced-air oven (SolidSteel, SSD 64L), divided into five 150 kg portions and manually cleaned of debris. The seeds were ground in a knife mill and sieved (0.8–5 mm). The comminuted material was impregnated with 1 M NaOH under constant stirring for 30 min, filtered and dried at 105°C for 24 h.

Pyrolysis was carried out at the Sanitary and Environmental Engineering Laboratory (LAESA, Federal University of Pará) in a batch reactor consisting of a 400 mL cylindrical stainless-steel vessel placed inside a 400 W electric furnace with a digital temperature controller (PID REX, C-100) and a K-type thermocouple. Approximately 200 g of impregnated material was heated at 10°C/min under atmospheric pressure to final temperatures of 350, 400 and 450°C. The vapours were routed through a 90° elbow to a straight stainless-steel condenser coupled to a thermostatic water recirculation system (SSDu 20L, 7Lab). The liquid product was collected, filtered and weighed to calculate the yield (bio-oil mass/initial biomass mass × 100), and its organic fraction was separated by filtration in a settling funnel and stored at room temperature, protected from light, until testing. The results of this study supported a patent application filed with the Brazilian National Institute of Industrial Property (INPI; BR 10 2025 029494 0).

2.2. Physicochemical characterisation

Density was measured at room temperature (20–25°C) with a 5 mL pycnometer (AOCS Cc 10c-95). The acid value was determined by dissolving 0.2 g of bio-oil in 50 mL of toluene/isopropanol (1:1, v/v) and titrating with standardised 0.1 N KOH, using phenolphthalein as indicator (AOCS Cd 3d-63); results are expressed as mg KOH/g. Kinematic viscosity was measured at 40°C with a Cannon-Fenske capillary viscometer (ASTM D2515).

2.3. Preparation of test solutions

Stock solutions of each bio-oil were prepared at 1000 µg/mL in DMSO 10% and serially diluted in the corresponding culture medium. The final vehicle concentration did not exceed 10% (v/v) in any assay, and a vehicle control at the highest concentration used was included in all experiments.

2.4. Cytotoxicity in skin cell lines

HaCaT human keratinocytes (300493; passage 39, 40, 41) and NIH-3T3 murine fibroblasts (CRL-1658; passage 37, 48, 55) were seeded at 2×10^4 cells/well in 96-well plates (TPP) in 200 µL of Dulbecco's modified Eagle medium (DMEM; Gibco) supplemented with 10% fetal bovine serum (FBS; Gibco), 2 mM L-glutamine (Sigma-Aldrich) and 1% antibiotic–antimycotic solution (10,000 U/mL penicillin, 10 mg/mL streptomycin and 25 µg/mL amphotericin B; A5955, Sigma-Aldrich), and allowed to adhere for 24 h at 37°C under 5% CO_2. Cells were then exposed for 24 h to the bio-oils (350, 400 and 450°C) at two-fold serial concentrations from 1000 to 1.95 µg/mL. Untreated cells in medium were used as the viability control and 50% (v/v) DMSO (Dinâmica Química) as the death control.

After treatment, the supernatant was discarded and the wells were washed three times with 200 µL of 0.9% NaCl. Then, 180 µL of phenol red-free DMEM and 20 µL of MTT (3-(4,5-dimethylthiazol-2-yl)-2,5-diphenyltetrazolium bromide; 5 mg/mL; Sigma-Aldrich) were added (final concentration 0.5 mg/mL) and the plates were incubated for 3 h in the dark. The formazan crystals were dissolved in 200 µL of DMSO and absorbance was read at 570 nm (SpectraMax M3, Molecular Devices). Viability was calculated as $(OD_{sample}/\text{mean } OD_{control}) \times 100$ (Ghasemi et al., 2021). Each condition was tested in triplicate in three independent experiments with different cell passages.

According to ISO 10993-5:2009, a reduction in viability greater than 30% is considered cytotoxic. Cytotoxicity was further graded as absent (> 80% viability), weak (60–80%), moderate (40–60%) or strong (< 40%) (López-García et al. 2014). The 50% cytotoxic concentration (CC_{50}) was calculated by four-parameter non-linear regression of log-transformed concentrations and is reported with its 95% confidence interval (Sebaugh 2011). The selectivity index (SI) was calculated as CC_{50}/MIC.

2.5. Bacterial strains and inoculum

Two reference strains were used: MRSA NCTC 12493 (*mecA*-positive) for the in vitro assays and *S. aureus* Rosenbach ATCC BAA-1026, oxacillin resistant, for the ex vivo assays. Strains were subcultured on Mueller-Hinton agar (MHA; Kasvi, K25-1058) for 24 h, and inocula were prepared in Mueller-Hinton broth (MHB; Kasvi, K25-1214) and adjusted spectrophotometrically at 625 nm (SP-2000UV, Spectrum) to the 0.5 McFarland standard (OD 0.09–0.11; ~1×10^8 CFU/mL), then diluted to 5×10^5 CFU/mL.

2.6. Minimum inhibitory and bactericidal concentrations

MIC was determined by broth microdilution according to CLSI M07 (CLSI 2018), with resazurin as growth indicator (Monteiro et al. 2012). In 96-well plates, 100 µL of inoculum and 100 µL of bio-oil at two-fold concentrations (1000–31.25 µg/mL) were combined. Controls included chloramphenicol (1 g/mL; Arifenicol, Blau Farmacêutica) as positive control, inoculum without treatment (growth control), 10% DMSO (vehicle control) and medium alone (sterility control). To exclude interference from the dark colour of the bio-oils, bio-oil dilutions without bacteria were incubated with resazurin in parallel. Plates were incubated for 24 h at 35°C, 20 µL of 0.01% resazurin (Sigma-Aldrich) was added and the plates were incubated for a further 3 h. The MIC was defined as the lowest concentration that prevented the colour change from blue to pink. For the MBC, 10 µL aliquots from the MIC well and from the wells with higher concentrations were plated on MHA and incubated for 24 h at 35°C; the MBC was defined as the lowest concentration that killed ≥ 99.9% of the initial inoculum (CLSI 1999; Quadros et al. 2011). Assays were performed in duplicate in 3 independent experiments.

2.7. Bacterial reactive oxygen species

Intracellular ROS were measured with 2',7'-dichlorodihydrofluorescein diacetate (H_2DCFH-DA) (Richard et al., 2002; Grasso et al. 2003; Zanghaei et al. 2023). An inoculum of MRSA NCTC 12493 (100 µL, 5×10^5 CFU/mL) was mixed with 100 µL of 520 mM tert-butyl hydroperoxide (TBHP; Sigma-Aldrich 416665) and incubated at 36°C for 60 min. Then, 100 µL of the 400°C bio-oil (final concentrations 125, 62.5, 31.25 and 15.62 µg/mL) was added and the mixture was incubated at 36°C for 120 min. Untreated bacteria (basal ROS) and bacteria + TBHP (oxidative stimulus) were used as controls. Ten microlitres of each mixture were transferred to a black 96-well plate containing 127 µL of reaction buffer, a blank reading was taken, and 10 µL of H_2DCFH-DA (216.47 µmol/L; Sigma-Aldrich D6883) was added. Fluorescence was read at 450 nm excitation and 525 nm emission (Synergy HTX, BioTek). To verify bacterial viability at the end of the assay, 10 µL of each mixture was plated on MHA and incubated for 24 h at 35°C.

2.8. Human organotypic skin explant culture (hOSEC)

Human skin was obtained from elective abdominoplasties of five donors (100% Women; age range 40–69 years; phototype I, II, III, V) who gave written informed consent for tissue donation. hOSEC was established as described by Frade et al. (2015) and Leite et al. (2021b). Immediately after surgery, skin was kept at 2–8°C for 4 h in PBS (Laborclin 590338) with 1.5% antibiotic–antimycotic solution (Sigma-Aldrich A5955). Subcutaneous fat was removed and the skin was cut into 8 mm (viability assays) and 10 mm (infection assays) fragments, which were placed dermis-side down on filter paper (80 g/m^2; air permeability 26 L/s·m^2; porosity 25 µm) supported by stainless-steel grids in 6-well plates containing 5 mL of DMEM with 10% FBS, 1% L-glutamine and 1% antibiotic–antimycotic, keeping the epidermis at the air–liquid interface. Explants were equilibrated for 24 h at 37°C under 5% CO_2.

2.9. Tissue viability

Two exposure routes were evaluated for 120 h at 37°C under 5% CO_2. (i) Dermal (medium) exposure: the medium was replaced with DMEM containing the 350, 400 or 450°C bio-oils (1000–1.95 µg/mL), renewed every 48 h. (ii) Topical exposure: based on the results of route (i), the 350°C bio-oil (125–1000 µg/mL) was applied onto the epidermal surface (10 µL per explant, reapplied every 48 h). DMEM-treated explants and 50% DMSO were used as viability and death controls, respectively. Viability was measured with 2,3,5-triphenyltetrazolium chloride (TTC) (De Lavor et al. 2015; Vostálová et al. 2018; Leite et al. 2021b; Souto-Silva et al. 2024). Explants were incubated in 1 mL of 2% TTC (Êxodo Científica TT07858RA) in phenol-free DMEM for 2 h at 37°C, washed with 0.9% NaCl, blotted dry and extracted overnight in 1.5 mL of DMSO/ethanol (1:1, v/v) at room temperature, protected from light and under agitation. Absorbance of 200 µL aliquots was read at 485 nm (SpectraMax M3), and viability was calculated relative to the DMEM control and classified as in Section 2.4.

2.10. Wounded hOSEC infection model and topical treatment

The colonisation model was performed as described by Lisboa et al. (2026). After 24 h of culture in antibiotic-free medium, a 4 mm wound was created in the centre of 10 mm explants with a dermatological punch and Castroviejo scissors, and 10 µL of a 10^6 CFU/mL suspension of *S. aureus* ATCC BAA-1026 (1×10^4 CFU/explant) was applied to the wound. Explants were incubated for 24 h at 37°C under 5% CO_2 to allow colonisation. Colonised explants then received a single topical application (10 µL) of 0.9% NaCl (negative control), 50% (v/v) antibiotic–antimycotic solution (positive control) or the 350, 400 or 450°C bio-oils at 500 and 1000 µg/mL. Explants from three donors were processed in triplicate and sampled immediately after treatment (0 h) and after 12 and 24 h. Bacteria were recovered with sterile swab (spreading) with 1 mL of 0.9% NaCl saline solution by simple streaks throughout the MHA plaque, serially diluted, and 10 µL was plated on MHA; colonies were counted after 24 h at 35°C. The limit of detection was 3 CFU/explant. Smears of the recovered suspensions were Gram-stained.

2.11. Statistical analysis

Data are presented as mean ± standard deviation (SD) or median and interquartile range (IQR), with individual values plotted. Normality was assessed with the Shapiro–Wilk test and residual plots. Parametric data were analysed by one-way analysis of variance (ANOVA) followed by Dunnett's test for comparisons with the control, or Tukey's test for all pairwise comparisons; non-parametric data were analysed by the Kruskal–Wallis test followed by Dunn's test. Bacterial counts were $\log_{10}$-transformed before analysis. Analyses were performed in GraphPad Prism 9 (GraphPad Software, San Diego, CA, USA), with significance set at $p < 0.05$.

3. Results

3.1. Physicochemical properties of the bio-oils

Bio-oil yield increased slightly with pyrolysis temperature, from 8.54% at 350°C to 8.84% at 400°C and 9.14% at 450°C (Table 1). The acid value decreased by approximately 62% between 350 and 450°C (from 40.84 to 15.51 mg KOH/g), whereas density increased from 1.016 to 1.078 g/mL. Kinematic viscosity ranged from 13.73 to 17.54 mm^2/s and was highest for the 400°C bio-oil (Table 2).

Table 1
Operating parameters of the pyrolysis of 1 M NaOH-impregnated açaí seeds

Parameter	350°C	400°C	450°C
Initial mass (g)	200.00	200.00	200.37
Pyrolysis time (min)	122	120	126
Onset temperature of condensation (°C)	266	258	337
Bio-oil mass (g)	17.09	17.67	18.32
Yield (%)	8.54	8.84	9.14
Yield = bio-oil mass/initial mass × 100.			

Table 2
Physicochemical properties of the açaí seed bio-oils

Parameter	350°C	400°C	450°C
Acid value (mg KOH/g)	40.84	27.46	15.51
Density (g/mL)	1.016	1.024	1.078
Kinematic viscosity at 40°C (mm^2/s)	13.73	17.54	15.25
Acid value: AOCS Cd 3d-63; density: AOCS Cc 10c-95; viscosity: ASTM D2515.			

3.2. Cytotoxicity in fibroblasts and keratinocytes

In the evaluation of cytotoxic effects by the MTT method (Fig. 1), was used NIH-3T3 fibroblasts (Fig. 1A-F) and HaCaT keratinocytes (Fig. 1G-L) treated for 24 h with açaí seed bio-oil impregnated with 1 M NaOH at different temperatures (350, 400, and 450°C) and concentrations ranging from 1000 to 1.95 µg/mL. All three bio-oils reduced the viability of NIH-3T3 fibroblasts in a concentration-dependent manner (Fig. 1A–F). At 250–1000 µg/mL, viability fell to 17–23.5% (strong cytotoxicity; $p < 0.0001$) regardless of pyrolysis temperature, and at 125 µg/mL it was 47.3–49.0% (moderate cytotoxicity; $p < 0.0001$). The 450°C bio-oil was also weakly cytotoxic at 62.5 µg/mL (74.3%; $p = 0.0268$). On the other hand, lower concentrations of bio-oils maintained viability and/or showed a proliferative effect at 15.6 µg/mL for the 400°C (148%; $p < 0.0001$) and 450°C (134%; $p = 0.0016$) bio-oils, and at 7.8 µg/mL for the 450°C bio-oil (129%; $p = 0.0088$). CC50 values decreased with pyrolysis temperature: 133.0, 130.4 and 115.5 µg/mL for the 350, 400 and 450°C bio-oils, respectively (Table 4).

Table 4
Cytotoxic concentrations (CC_{50}) and selectivity indices (SI = CC_{50}/MIC) of açaí seed bio-oils

Bio-oil	CC_{50} NIH-3T3 (µg/mL)	CC_{50} HaCaT (µg/mL)	CC_{50} hOSEC[a] (µg/mL)	SI 3T3	SI HaCaT	SI hOSEC
350°C	133.0	305.3	> 1000	0.13	0.31	> 1
400°C	130.4	184.4	> 1000	0.26	0.37	> 2
450°C	115.5	170.2	> 1000	0.23	0.34	> 2

[a] Dermal (medium) exposure for 120 h; viability remained > 50% at the highest concentration tested (1000 µg/mL). Add 95% confidence intervals after refitting the curves.

HaCaT keratinocytes were less sensitive (Fig. 1G–L). At 500 and 1000 µg/mL, all bio-oils were strongly cytotoxic (20–25% viability; $p < 0.0001$). At 250 µg/mL, the 350°C bio-oil was moderately cytotoxic (57%), whereas the 400 and 450°C bio-oils were strongly cytotoxic (28% and 27%; $p < 0.0001$). At 125 µg/mL, the 400 and 450°C bio-oils were weakly cytotoxic (61.75% for both; $p < 0.0001$), as was the 450°C bio-oil at 62.5 µg/mL (76.5%; $p = 0.0015$). The lowest concentrations of bio-oil at 350ºC exhibited a proliferative effect at 1.95 µg/mL (130%) and 3.9 µg/mL (136%) ($p < 0.0001$) and for the 400°C bio-oil at 62.5 µg/mL (124%; $p = 0.0149$), but not for the 450°C bio-oil. CC_{50} values were 305.3, 184.4 and 170.2 µg/mL for the 350, 400 and 450°C bio-oils, respectively (Table 4).

3.3. Antibacterial activity against MRSA

All bio-oils inhibited the growth of MRSA NCTC 12493 (Fig. 2; Table 3). The MIC and MBC were 1000 µg/mL for the 350°C (Fig. 2-A) bio-oil and 500 µg/mL for the 400 (Fig. 2-B) and 450°C (Fig. 2-C) bio-oils; no colonies were recovered from the MIC wells (median 0 [IQR 0–0] colonies), as with chloramphenicol (1 g/mL; median = 0; IQR: 0–0 CFU). The growth and vehicle (10% DMSO) controls produced confluent growth (> 1000 colonies per plate (IQR: 1000–1000); Fig. 2-D). Because the MICs exceeded the monolayer CC_{50} values, the SI calculated with fibroblast and keratinocyte data was below 1 (0.13–0.37), whereas the SI calculated with hOSEC data was above 1 (Table 4).

Table 3
Minimum inhibitory (MIC) and bactericidal (MBC) concentrations of açaí seed bio-oils against MRSA NCTC 12493

Bio-oil	MIC (µg/mL)	MBC (µg/mL)	MBC/MIC	Activity[a]
350°C	1000	1000	1	Weak
400°C	500	500	1	Moderate
450°C	500	500	1	Moderate

[a] Classification for natural products according to Kuete (2010): significant, MIC < 100 µg/mL; moderate, 100–625 µg/mL; weak, > 625 µg/mL. MBC/MIC ≤ 4 indicates bactericidal activity.

3.4. Bacterial reactive oxygen species

In the evaluation of oxidative stress associated with the experimental treatments (Fig. 3), untreated MRSA showed basal DCF fluorescence of 181 A.U. (SD: 38.97), which increased to 311 A.U. (SD: 19.31) after TBHP stimulation ($p = 0.0001$; Fig. 3-A). Exposure of TBHP-stimulated bacteria to the 400°C bio-oil reduced fluorescence to 34 A.U. (SD: 17.69; $p < 0.0001$) at 125 µg/mL, 34.3 A.U. (SD: 21.83) at 62.5 µg/mL and 61.66 A.U. (SD: 11.37; $p = 0.0002$) at 31.25 µg/mL, values lower than those of both the basal and TBHP-stimulated groups ($p < 0.0001$). At 15.62 µg/mL, fluorescence (mean: 166.33 A.U.; SD: 23.63) did not differ from the basal level but remained lower than that of the TBHP group. When aliquots were plated at the end of the assay, no colonies were recovered at any bio-oil concentration (median 0 [IQR 0–0]), whereas the TBHP-only control showed bacterial growth (Fig. 3-B). Thus, under oxidative stress, the bio-oil was bactericidal at concentrations well below its MIC.

3.5. Tolerability in human skin explants

After 120 h of dermal (medium) exposure (Fig. 4), the 350°C (Fig. 4-A) bio-oil maintained mean tissue viability above 80% at all concentrations (86.5–100%; CC_{50} > 1000 µg/mL; Fig. 4-D). The 400°C (Fig. 4-B) bio-oil reduced viability to 79.20% (SD: 6.49) at 500 µg/mL (weak cytotoxicity; $p < 0.05$) and 53% (SD: 12.35) at 1000 µg/mL (moderate; $p < 0.05$), with viability close to or above 80% at lower concentrations. The 450°C (Fig. 4-C) bio-oil was not cytotoxic at 500 µg/mL (84.25%; SD: 10.81) and weakly cytotoxic at 1000 µg/mL (61.2 ± 6.38%; $p < 0.05$). Because viability remained above 50% at the highest concentration tested, the CC_{50} of all bio-oils was > 1000 µg/mL (curve-fit extrapolations: 1440 µg/mL for 400°C (Fig. 4-E) and 5640 µg/mL for 450°C (Fig. 4-F).

Owing to its more favourable profile, the 350°C bio-oil was selected for topical exposure (Fig. 5). Topical application did not significantly reduce viability compared with DMEM: median viability was 81% (IQR 78–95%) at 1000 µg/mL, 75% (IQR 73–81%) at 500 µg/mL (weak cytotoxicity) and above 80% at 250 and 125 µg/Ml (Fig. 5-A), with a CC_{50} of 1,710 µg/mL (Fig. 5-B).

3.6. Antibacterial activity in the wounded hOSEC model

Bacterial counts are expressed as colony counts, as plotted in Fig. 6. Immediately after treatment (0 h), counts in all groups exceeded the upper limit of quantification (> 1000 colonies), confirming homogeneous colonization (Fig. 6-A).

At 12 h (Fig. 6-B), the antibiotic–antimycotic control showed the lowest counts (mean ≈ 14 colonies; SD: 0), compared with mean ≈ 388.7 (SD: 0) in the saline group. Among the bio-oils, the 450°C bio-oil at 1000 µg/mL produced the lowest counts (mean ≈ 49.5; SD: 0), 89% lower than the same bio-oil at 500 µg/mL (mean ≈ 460.3; SD: 0). Counts for the 350°C (500 µg/mL: mean ≈ 900, SD: 0; 1000 µg/mL: mean ≈ 650.3, SD: 0) and 400°C bio-oils (500 µg/mL: mean ≈ 1000, SD: 0; 1000 µg/mL: mean ≈ 943.5, SD: 0) remained high. No bio-oil group differed significantly from the antibiotic control at this time point.

At 24 h (Fig. 6-C), counts were 24.1 in the antibiotic group and ≈ 24 colonies (SD: 0) in the saline group. The 350°C and 450°C bio-oils at 1000 µg/mL reduced counts to near the detection limit (median 0 [IQR 0–1] for both), significantly lower than the antibiotic control ($p = 0.0483$ and $p = 0.0446$, respectively). The 400°C bio-oil yielded intermediate counts (500 µg/mL: mean ≈ 56.0, SD: 0; 1000 µg/mL: mean ≈ 17.8, SD: 0). In contrast, at 500 µg/mL the 350°C (mean ≈ 437.5, SD: 0) and 450°C (mean ≈ 328.0, SD: 0) bio-oils did not reduce colonisation. Representative plates and Gram-stained smears are shown in Fig. 6-D.

4. Discussion

This study shows that bio-oil obtained by pyrolysis of NaOH-impregnated açaí seeds is bactericidal against MRSA and that, although cytotoxic to keratinocytes and fibroblasts in monolayer at concentrations below the MIC, it is well tolerated by human skin explants, in which a single topical application at 1000 µg/mL nearly eliminated *S. aureus* from a wound within 24 h. These findings support the use of the wounded hOSEC model to bridge the gap between monolayer screening and in vivo testing of topical antimicrobials.

The slight increase in yield with temperature agrees with previous reports for açaí seeds, which ranged from 4.37% to 13.09% (De Castro et al. 2021) and from 3.19% to 6.79% between 350 and 450°C (Valois et al. 2024), and reflects more efficient thermal degradation of the lignocellulosic matrix at higher temperatures (Baia 2022). Hemicellulose and cellulose decompose mainly between 200 and 400°C, whereas lignin degrades over a wider range and is the main source of phenolic and aromatic compounds; as temperature increases, the oxygenated fraction decreases and aromatic hydrocarbons increase (Abnisa et al. 2013; Bridgwater 2012; Valois et al. 2024). The ~ 62% reduction in acid value between 350 and 450°C is consistent with a lower content of carboxylic acids at higher temperatures and with the value reported by Valois et al. (2024) at 450°C. For topical use, a lower acid value is desirable, because acidity can compromise formulation stability, excipient compatibility and skin tolerance (Sinko 2011). Densities were close to those reported for açaí seed bio-oil (1.043 g/mL; De Castro et al. 2021) and palm empty fruit bunch bio-oil (1.030 g/mL; Abnisa et al. 2013), and viscosities were lower than those of bio-oils from corn stover (148 mm^2/s; Yu et al. 2007) and açaí seeds without

fractionation (68.34 mm^2/s; De Castro et al. 2021), which favours incorporation into topical formulations.

In monolayers, the bio-oils were cytotoxic in a concentration-dependent manner, and fibroblast CC_{50} decreased slightly as pyrolysis temperature increased, in line with the higher toxicity reported for açaí seed bio-oils produced at higher temperatures (Silva et al. 2024a). Phenols and other lipophilic constituents of bio-oil can partition into cell membranes and disrupt their integrity, and their effects are attenuated at low concentrations (Valdez et al. 2023). The MTT signal above 100% observed at low concentrations should be interpreted with caution: MTT reduction reflects mitochondrial and cytosolic reductase activity and may increase without a corresponding increase in cell number (Ghasemi et al. 2021). This hormetic-like response therefore indicates increased metabolic activity rather than proliferation, which would require confirmation by cell counting or DNA-based assays.

The MIC/MBC values of 500–1000 µg/mL correspond to moderate (400 and 450°C) and weak (350°C) activity according to the criteria used for crude natural products (Ríos and Recio, 2005; Kuete, 2010), and the MBC/MIC ratio of 1 indicates bactericidal rather than bacteriostatic action. These values cannot be compared directly with clinical breakpoints, which apply to pure antibiotics; for reference, the EUCAST susceptibility breakpoint for chloramphenicol against *S. aureus* is 8 mg/L (EUCAST 2025), about 60 times lower than the MIC of the most active bio-oils. Activity was greater for the bio-oils produced at higher temperatures, consistent with previous observations that temperature is a key determinant of the antimicrobial activity of açaí seed bio-oil (Silva et al. 2024a) and with the enrichment of phenolic compounds as oxygenated compounds decrease (Valdez et al. 2023; Valois et al. 2024). Nevertheless, the difference between 350°C and 400/450°C corresponds to a single two-fold dilution, which is within the expected variability of broth microdilution, and the compounds responsible for the activity remain to be identified.

TBHP-stimulated MRSA exposed to the 400°C bio-oil showed lower DCF fluorescence than both unstimulated and TBHP-stimulated bacteria. One interpretation is that phenolic constituents scavenge radicals and modulate bacterial redox pathways (Lopez-Romero et al. 2015; Barbarossa et al. 2025), counteracting the oxidative challenge to which *S. aureus* normally responds with catalase-dependent adaptation (Linzner et al. 2022). However, no colonies were recovered after the assay at any bio-oil concentration, including 15.62 µg/mL, which is 32 times below the MIC. Because H_2DCFH-DA must be deacetylated by intracellular esterases to generate a fluorescent signal, loss of viability can by itself reduce fluorescence, and phenolic compounds may also react directly with the probe or quench DCF fluorescence (Kalyanaraman et al. 2012). The fact that fluorescence at 15.62 µg/mL returned to basal levels despite the absence of growth suggests that the reduction in fluorescence at higher concentrations is not explained by viability loss alone. More importantly, the bactericidal effect at sub-MIC concentrations in the presence of TBHP suggests that oxidative stress and the bio-oil act cooperatively, a hypothesis that deserves further investigation. To our knowledge, antioxidant activity of açaí seed bio-oil had only been assessed in cell-free systems (TEAC and DPPH; Valois et al. 2024; Silva et al. 2024a); this is the first evaluation in bacteria.

A central finding of this study is the discrepancy between monolayer and tissue toxicity. Bio-oil concentrations that reduced HaCaT and NIH-3T3 viability below 25% after 24 h were tolerated by skin explants for 120 h, especially for the 350°C bio-oil, which kept viability above 80% at all concentrations when added to the medium or applied topically. In monolayers, cells are directly exposed to the test substance, whereas in skin the stratum corneum, the extracellular matrix and cell–cell interactions limit the amount of compound that reaches viable cells (Proksch et al. 2008). Consequently, the selectivity index, which was below 1 in monolayers, rose above 1 in hOSEC. For topical products, the tissue-based index is the more relevant estimate of the therapeutic window, and these data indicate that bactericidal concentrations can be applied to human skin without substantial tissue damage.

In the wounded hOSEC model, a single application of the 350°C and 450°C bio-oils at 1000 µg/mL reduced *S. aureus* counts to near the detection limit within 24 h, below those obtained with the antibiotic–antimycotic control. This comparison should be interpreted with caution, because penicillin and streptomycin are not expected to be fully active against a resistant strain; a clinically used topical agent such as mupirocin or fusidic acid would be a more appropriate comparator. The effect was concentration-dependent: at 500 µg/mL, which corresponds to the in vitro MIC of the 400 and 450°C bio-oils, counts remained similar to or higher than those of the saline group, indicating that concentrations above the MIC are required in tissue, probably because of binding to tissue components and limited diffusion into the wound bed. Unlike in vitro, activity in tissue did not increase monotonically with pyrolysis temperature, as the 400°C bio-oil was less effective at 12 and 24 h; it is tempting to relate this to its higher viscosity, which could limit diffusion, but this hypothesis requires testing.

The hOSEC model preserves keratinocytes, melanocytes, Langerhans cells, fibroblasts, the extracellular matrix and the dermo-epidermal junction, and therefore integrates microbiological and tissue-level outcomes that 2D and reconstructed 3D models cannot fully capture (Lebonvallet et al. 2010; Masson-Meyers et al. 2020; Barua et al. 2021; Rikken et al. 2023). It also avoids the use of animals and reflects the genetic diversity of human donors (Frade et al. 2015; Leite et al. 2021b; Lopes 2022; De Paula et al. 2024; Souto-Silva et al. 2024). Future studies using this platform should include histopathology, cytokine and antimicrobial peptide profiling and ROS measurement in tissue to clarify how the bio-oil, the cutaneous immune response and bacterial clearance interact.

This study has limitations. First, the chemical composition of the bio-oils was not determined; GC–MS profiling and quantification of phenolics and polycyclic aromatic hydrocarbons, which can occur in pyrolysis liquids (Bridgwater 2012), are needed to identify active constituents and to assess safety before topical use. Second, each bio-oil was produced in a single pyrolysis batch, so batch-to-batch variability was not assessed. Third, different strains were used in vitro (NCTC 12493) and ex vivo (ATCC BAA-1026), because the MRSA strain could not be maintained in the explant model, and MIC/MBC were determined for only one strain. Fourth, the antibiotic–antimycotic control is not a clinically relevant comparator for MRSA. Fifth, the dark colour of the bio-oils may interfere with colorimetric and fluorimetric readouts, and the ROS assay lacked cell-free controls and normalisation to viable bacteria. Sixth, counts in the saline group decreased spontaneously between 12 and 24 h, and the number of

donors was small, which limits statistical power; donor-related differences in skin thickness and structure may contribute to variability. Finally, the explant model lacks circulation, recruitment of immune cells and a resident microbiota.

5. Conclusions

Bio-oils produced by pyrolysis of NaOH-impregnated açaí seeds at 350, 400 and 450°C were bactericidal against MRSA, with MIC and MBC of 500 µg/mL for the 400 and 450°C bio-oils and 1000 µg/mL for the 350°C bio-oil. Although cytotoxic to keratinocytes and fibroblasts in monolayer at concentrations of 125 µg/mL and above, the bio-oils were well tolerated by human skin explants: the 350°C bio-oil maintained tissue viability above 80% at all concentrations, and the 400 and 450°C bio-oils reduced viability to 53% and 61%, respectively, only at 1000 µg/mL. In TBHP-stressed bacteria, the 400°C bio-oil reduced DCF fluorescence and was bactericidal at sub-MIC concentrations. In the wounded hOSEC model, the 350 and 450°C bio-oils at 1000 µg/mL reduced *S. aureus* counts to near the detection limit within 24 h. Together, these results identify açaí seed bio-oil as a promising source of topical antibacterial compounds and show the value of the wounded hOSEC model as a human-relevant, animal-free platform for testing them. Chemical characterisation, formulation and comparison with clinically used topical antibiotics are the next steps toward application, which would also add value to an abundant Amazonian agro-industrial residue.

CRediT authorship contribution statement

L.F.T.L., F.R.L., and M.C.M. contributed to conceptualization and methodology. L.F.T.L., C.V.S.G., L.H.H.G., and F.R.L. contributed to investigation. L.F.T.L. and F.R.L. contributed to formal analysis and writing – original draft. L.H.H.G., N.T.M., M.A.C.F., F.R.L., P.S.C., and E.P.P. contributed to resources. N.T.M., M.A.C.F., F.R.L., and M.C.M. contributed to supervision. M.C.M. contributed to funding acquisition. C.V.S.G., L.H.H.G., N.T.M., M.A.C.F., F.R.L., M.C.M., P.S.C., and E.P.P. contributed to writing – review & editing.

Declarations

Declaration of competing interest

The authors declare that they have no known competing financial interests or personal relationships that could have appeared to influence the work reported in this paper. A patent application related to this work has been filed with INPI (BR 10 2025 029494 0).

Ethics statement

The Institutional Review Board for Human Research of the Hospital of the Ribeirão Preto Medical School – University of São Paulo approved the study (CAAE: 82939424.4.3001.5440, number: 7.208.516; approved on 06/11/2024); as well as the Research Ethics Committee of the Federal University of Pará (CAAE: 82939424.4.1001.0018, number: 7.198.616; approved on 01/11/2024), in accordance with the Declaration of Helsinki. The patients/participants provided their written informed consent to have their data analyzed.

Declaration of generative AI use

The authors declare that they used the Generative Artificial Intelligence tool [ChatGPT], version 5.3, for language revision and improvement of grammar, spelling, clarity, and writing style. All content has been reviewed, and the authors assume full responsibility for the integrity and accuracy of the information presented in the final manuscript.

Role of the funding source

The study's funder had no role in the design, data collection, analysis, interpretation, or writing of the report. All authors had full access to all the data in the study and had final responsibility for the decision to submit for publication.

Funding

This research was funded by the National Council for Scientific and Technological Development (CNPq), the Coordination for the Improvement of Higher Education Personnel (CAPES), the Amazon Foundation for the Support of Research (FAPESPA), the Federal University of Pará (UFPA), and the Foundation for the Support of Teaching, Research, and Assistance of the Hospital das Clínicas of the Ribeirão Preto Medical School, University of São Paulo (FAEPA). We also thank INCT-PROBIAM Pharmaceuticals Amazônia (Grant No. 406819/2022-0) and SUSTENBIO (Grant No. 405886/2022-5) for their support. This work was also supported by the Office of the Pro-Rector for Research and Graduate Studies at UFPA (PROPESP-UFPA, Brazil) through funding for open-access publication fees. MCM holds a research productivity fellowship from CNPq. The Article Processing Charge (APC) for this publication was funded by the Coordination for the Improvement of Higher Education Personnel (CAPES), Brazil – Finance Code 001.

Author Contribution

L.F.T.L., F.R.L., and M.C.M. contributed to conceptualization and methodology. L.F.T.L., C.V.S.G., L.H.H.G., and F.R.L. contributed to investigation. L.F.T.L. and F.R.L. contributed to formal analysis and writing – original draft. L.H.H.G., N.T.M., M.A.C.F., F.R.L., P.S.C., and E.P.P. contributed to resources. N.T.M., M.A.C.F., F.R.L., and M.C.M. contributed to supervision. M.C.M. contributed to funding acquisition.

C.V.S.G., L.H.H.G., N.T.M., M.A.C.F., F.R.L., M.C.M., P.S.C., and E.P.P. contributed to writing – review & editing.

Acknowledgement

We thank the team members and all patients who participated in this study. We also thank INCT-PROBIAM Pharmaceuticals Amazônia for the partnership and collaboration in the development of this work.

Data Availability

All data generated or analyzed during this study are included in this published article.

References

1. Abnisa F, Arami-Niya A, Daud WMAW, Sahu JN (2013) Characterization of bio-oil and bio-char from pyrolysis of palm oil wastes. BioEnergy Res 6:830–840
2. Avelino TM, Harb SV, Adamoski D et al (2024) Unveiling the impact of hypodermis on gene expression for advancing bioprinted full-thickness 3D skin models. Commun Biol 7:1437. https://doi.org/10.1038/s42003-024-07106-4
3. Baia ACF (2022) Study of the pyrolysis of açaí (*Euterpe oleracea*Mart.) seeds at pilot scale for biofuel production [in Portuguese]. Master's dissertation, Federal University of Pará, Belém
4. Barbarossa A, Argentieri MP, Diella MV et al (2025) Exploring the antibacterial, anti-inflammatory, and antioxidant properties of the natural food supplement Protegol as a supportive strategy in respiratory tract infections. Antibiotics 14:1260. https://doi.org/10.3390/antibiotics14121260
5. Barua N, Huang L, Li C et al (2021) Comparative study of two-dimensional (2D) vs. three-dimensional (3D) organotypic keratinocyte-fibroblast skin models for *Staphylococcus aureus* (MRSA) infection. Int J Mol Sci 23:299. https://doi.org/10.3390/ijms23010299
6. Bridgwater AV (2012) Review of fast pyrolysis of biomass and product upgrading. Biomass Bioenergy 38:68–94
7. Cheung GYC, Bae JS, Otto M (2021) Pathogenicity and virulence of *Staphylococcus aureus*. Virulence 12:547–569. https://doi.org/10.1080/21505594.2021.1878688
8. CLSI (1999) Methods for Determining Bactericidal Activity of Antimicrobial Agents; Approved Guideline. CLSI document M26-A. Clinical and Laboratory Standards Institute, Wayne, PA
9. CLSI (2018) Methods for Dilution Antimicrobial Susceptibility Tests for Bacteria That Grow Aerobically, 11th ed. CLSI standard M07. Clinical and Laboratory Standards Institute, Wayne, PA
10. COSTA FG, MILLS KB, CROSBY HA (2024) HORSWILL AR The *Staphylococcus aureus*regulatory program in a human skin-like environment. mBio. May 8;15(5):e 045324. 10.1128/mbio.00453-24

11. Da Silva AKA, Nunes GAMA, Faria RM et al (2026) Advanced microfluidic and 3D cell culture platforms for modeling vascularization in diabetic foot ulcers: a systematic review of translational challenges and perspectives. PLoS ONE 21:e0328278. https://doi.org/10.1371/journal.pone.0328278
12. De Barros NR, Harb SV, Horinouchi CDS, Tofani LB et al (2025) Advances in 3D bioprinting and microfluidics for organ-on-a-chip platforms. Polymers 17:3078. https://doi.org/10.3390/polym17223078
13. De Castro DAR, Ribeiro HJS, Guerreiro LHH et al (2021) Production of fuel-like fractions by fractional distillation of bio-oil from açaí (*Euterpe oleracea* Mart.) seeds pyrolysis. Energies 14:3713
14. De Lavor MS, Binda NS, Fukushima FB et al (2015) Ischemia-reperfusion model in rat spinal cord: cell viability and apoptosis signaling study. Int J Clin Exp Pathol 8:9941–9949
15. De Paula NA, Leite MN, de Faria Bertoluci DF et al (2024) Human skin as an ex vivo model for the maintenance of *Mycobacterium leprae* and leprosy studies. Trop Med Infect Dis 9:135. https://doi.org/10.3390/tropicalmed9060135
16. Dias-Souza MV, dos Santos RM, Cerávolo IP, Cosenza G, Ferreira Marçal PH, Figueiredo FJB (2018) *Euterpe oleracea* pulp extract: chemical analyses, antibiofilm activity against *Staphylococcus aureus*, cytotoxicity and interference on the activity of antimicrobial drugs. Microb Pathog 114:29–35
17. EUCAST (2025) Breakpoint tables for interpretation of MICs and zone diameters, version 15.0. European Committee on Antimicrobial Susceptibility Testing. https://www.eucast.org
18. FDA (2026) FDA releases draft guidance on alternatives to animal testing in drug development. U.S. Food and Drug Administration. https://www.fda.gov/news-events/press-announcements(accessed 24 April 2026)
19. Feitoza US, Thue PS, Lima EC et al (2022) Use of biochar prepared from the açaí seed as adsorbent for the uptake of catechol from synthetic effluents. Molecules 27(21)
20. Frade MAC, Andrade TAM, Aguiar AFCL et al (2015) Prolonged viability of human organotypic skin explant in culture method (hOSEC). Bras Dermatol 90:347–350
21. Ghasemi M, Turnbull T, Sebastian S, Kempson I (2021) The MTT assay: utility, limitations, pitfalls, and interpretation in bulk and single-cell analysis. Int J Mol Sci 22:12827. https://doi.org/10.3390/ijms222312827
22. Grasso S, Scifo C, Cardile V et al (2003) Adaptive responses to the stress induced by hyperthermia or hydrogen peroxide in human fibroblasts. Exp Biol Med 228:491–498. https://doi.org/10.1177/15353702-0322805-12
23. ISO (2009) ISO 10993-5:2009. Biological Evaluation of Medical Devices – Part 5: Tests for In Vitro Cytotoxicity. International Organization for Standardization, Geneva
24. Kalyanaraman B, Darley-Usmar V, Davies KJA et al (2012) Measuring reactive oxygen and nitrogen species with fluorescent probes: challenges and limitations. Free Radic Biol Med 52:1–6
25. Kuete V (2010) Potential of Cameroonian plants and derived products against microbial infections: a review. Planta Med 76:1479–1491

26. Lebonvallet N, Jeanmaire C, Danoux L et al (2010) The evolution and use of skin explants: potential and limitations for dermatological research. Eur J Dermatol 20:671–684
27. Leite MN (2021a) Validation of the ex vivo human skin model (hOSEC) for absorption assays of pharmaceutical ingredients [in Portuguese]. PhD thesis, University of São Paulo, Ribeirão Preto
28. Leite MN, Viegas JSR, Praça FSG et al (2021b) Ex vivo model of human skin (hOSEC) for assessing the dermatokinetics of the anti-melanoma drug dacarbazine. Eur J Pharm Sci 160:105769. https://doi.org/10.1016/j.ejps.2021.105769
29. Linzner N, Loi VV, Antelmann H (2022) The catalase KatA contributes to microaerophilic H_2O_2 priming to acquire an improved oxidative stress resistance in *Staphylococcus aureus*. Antioxidants 11:1793. https://doi.org/10.3390/antiox11091793
30. Lisboa LFT, Barbosa LD, Giarola F et al (2026) Human Organotypic Skin Explant Culture (hOSEC): An Alternative translational Approach to *Staphylococcus aureus* Colonization Assays. Int Microbiol. https://doi.org/10.1007/s10123-026-00908-y
31. Lopes MAR (2022) Assessment of the viability and application of the ex vivo human skin model (hOSEC) for photoaging studies. Master's dissertation, University of São Paulo, Ribeirão Preto. https://doi.org/10.11606/D.17.2022.tde-01122022-120850
32. López-García J, Lehocký M, Humpolíček P, Sáha P (2014) HaCaT keratinocytes response on antimicrobial atelocollagen substrates: extent of cytotoxicity, cell viability and proliferation. J Funct Biomater 5:43–57
33. Lopez-Romero JC, González-Ríos H, Borges A, Simões M (2015) Antibacterial effects and mode of action of selected essential oils components against *Escherichia coli* and *Staphylococcus aureus*. Evid Based Complement Alternat Med 795435
34. Magalhães TSSA, de Oliveira Macedo PC, da Costa ÉCP et al (2021) Increase in the antioxidant and anti-inflammatory activity of *Euterpe oleracea* Martius oil complexed in β-cyclodextrin and hydroxypropyl-β-cyclodextrin. Int J Mol Sci 22:11524
35. Masson-Meyers DS, Andrade TAM, Caetano GF et al (2020) Experimental models and methods for cutaneous wound healing assessment. Int J Exp Pathol 101:21–37
36. Monge-Fuentes V, Muehlmann LA, Longo JPF et al (2017) Photodynamic therapy mediated by acai oil (*Euterpe oleracea* Martius) in nanoemulsion: a potential treatment for melanoma. J Photochem Photobiol B 166:301–310
37. Monteiro MC, de la Cruz M, Cantizani J et al (2012) A new approach to drug discovery: high-throughput screening of microbial natural extracts against *Aspergillus fumigatus* using resazurin. J Biomol Screen 17:542–549
38. Murray CJL, Ikuta KS, Sharara F et al (2022) Global burden of bacterial antimicrobial resistance in 2019: a systematic analysis. Lancet 399:629–655
39. Nobre JRC et al (2023) Potential of agro-industrial residues from the Amazon region to produce activated carbon. Heliyon 9:e17189. https://doi.org/10.1016/j.heliyon.2023.e17189

40. Pedro DA (2021) Alternative methods to animal use in teaching and research: evolution and current overview in Brazil [in Portuguese]. Enciclopédia Biosfera 18(37)
41. Proksch E, Brandner JM, Jensen JM (2008) The skin: an indispensable barrier. Exp Dermatol 17:1063–1072
42. Quadros AU, Bini D, Pereira PAT et al (2011) Antifungal activity of some cyclooxygenase inhibitors on *Candida albicans*: PGE2-dependent mechanism. Folia Microbiol 56:349–352. https://doi.org/10.1007/s12223-011-0049-6
43. Richard D, Hollender P, Chénais B (2002) Involvement of reactive oxygen species in aclarubicin-induced differentiation and invasiveness of HL-60 leukemia cells. Int J Oncol 21:393. https://doi.org/10.3892/ijo.21.2.393
44. Rikken G, Meesters LD, Jansen PAM et al (2023) Novel methodologies for host-microbe interactions and microbiome-targeted therapeutics in 3D organotypic skin models. Microbiome 11:227. https://doi.org/10.1186/s40168-023-01668-x
45. Ríos JL, Recio MC (2005) Medicinal plants and antimicrobial activity. J Ethnopharmacol 100:80–84
46. Sebaugh JL (2011) Guidelines for accurate EC50/IC50 estimation. Pharm Stat 10:128–134
47. Shaaban MT, Orabi SH, Abdel-Hamid MS et al (2024) Therapeutic potential of green-synthesized silver nanoparticles: combating biofilms of multidrug-resistant *Staphylococcus aureus*. Vet World 17:456–462
48. Silva IC et al (2024a) Effect of temperature and molarity on the antimicrobial, cytotoxic and antioxidant activities of açaí (*Euterpe oleracea*Mart.) seed bio-oil [in Portuguese]
49. Sinko PJ (2011) Martin's Physical Pharmacy and Pharmaceutical Sciences, 6th edn. Lippincott Williams & Wilkins, Philadelphia
50. Sousa JL, Guerreiro LHH, Bernar LP et al (2021) Chemical analysis of bio-oil produced by pyrolysis of açaí (*Euterpe oleracea* Mart.) seeds. Braz J Dev 7:15549–15565
51. Souto-Silva MV, Bispo ECI, Albuquerque LFF et al (2024) Toxicity and dermatokinetic analysis of ibrutinib in human skin models. Pharmaceutics 16:1377. https://doi.org/10.3390/pharmaceutics16111377
52. Tong SYC, Davis JS, Eichenberger E, Holland TL, Fowler VG (2015) *Staphylococcus aureus* infections: epidemiology, pathophysiology, clinical manifestations, and management. Clin Microbiol Rev 28:603–661
53. Valdez GD et al (2023) Improving the bio-oil quality of residual biomass pyrolysis by chemical activation: effect of alkalis and acid pre-treatment. Energies 16(7)
54. Valois FP et al (2024) Improving the antioxidant activity, yield, and hydrocarbon content of bio-oil from the pyrolysis of açaí seeds by chemical activation: effect of temperature and molarity. Catalysts 14:44
55. Vostálová J, Cukr M, Ulrichová J et al (2018) Comparison of various methods to analyse toxic effects in human skin explants: rediscovery of TTC assay. J Photochem Photobiol B 178:530–536

56. Wu X et al (2026) Reimagining human-centric drug development with new approach methodologies. Science 392:371–378. https://doi.org/10.1126/science.aeb0045
57. Yu F, Deng S, Chen P et al (2007) Physical and chemical properties of bio-oils from microwave pyrolysis of corn stover. Appl Biochem Biotechnol 136–140:957–970
58. Zanghaei A et al (2023) Rapid identification of bacteria by the pattern of redox reactions rate using 2',7'-dichlorodihydrofluorescein diacetate. Biochem Biophys Res Commun 678:78–83. https://doi.org/10.1016/j.bbrc.2023.08.026

Figures

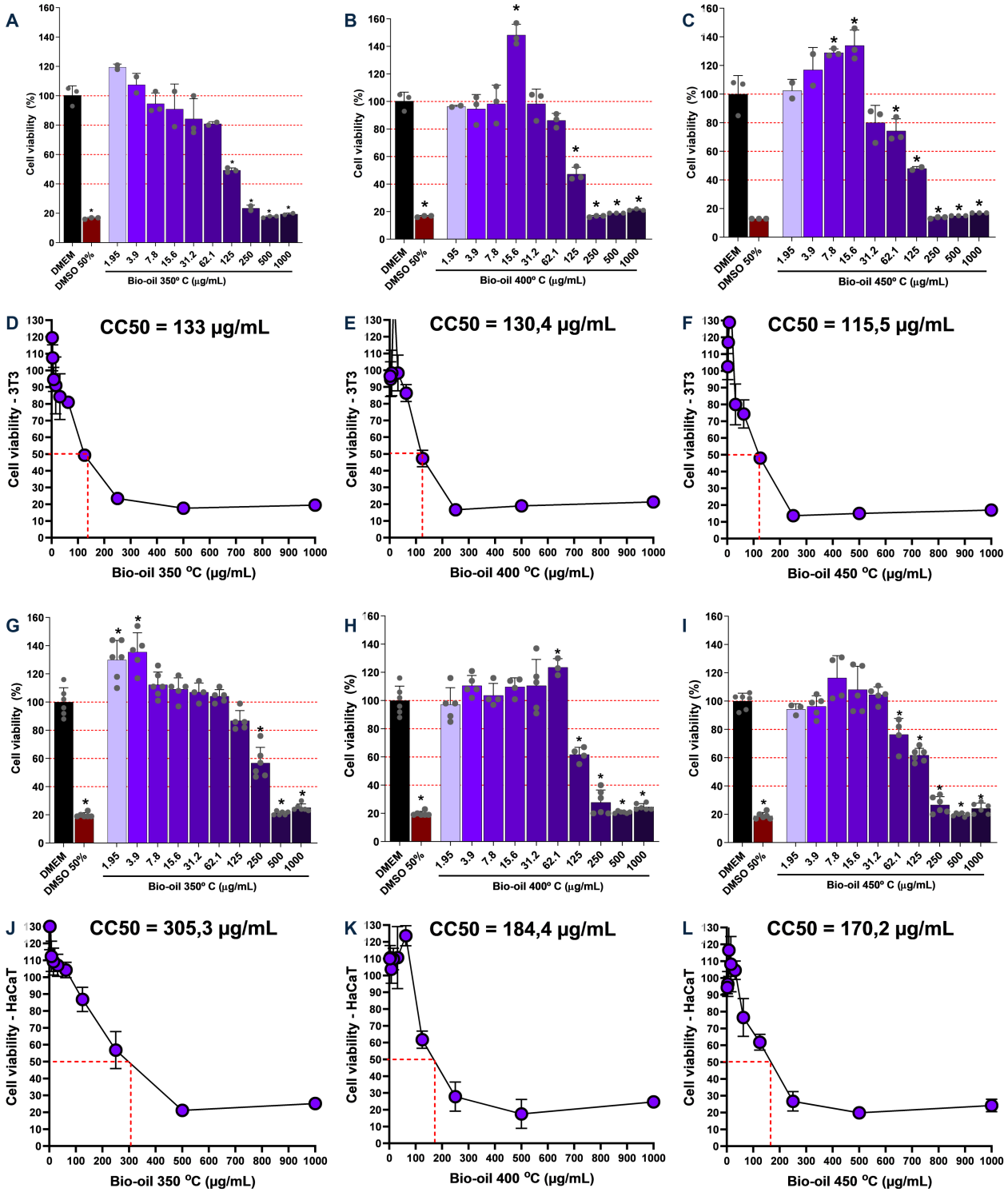


Figure 1

Cytotoxicity of açaí seed bio-oils in skin cell lines. Viability of NIH-3T3 fibroblasts (A–C) and HaCaT keratinocytes (G–I) after 24 h of exposure to bio-oils produced from 1 M NaOH-impregnated seeds at 350 °C (A, G), 400 °C (B, H) and 450 °C (C, I) (1.95–1000 µg/mL), measured by the MTT assay. Concentration–response curves and CC_{50} values for NIH-3T3 (D–F) and HaCaT cells (J–L). Data are mean ± SD with individual values. Dashed red lines indicate the cytotoxicity thresholds (80%, 60% and

40% viability). DMEM, viability control; 50% DMSO, death control. *p < 0.05 vs. DMEM (one-way ANOVA followed by Dunnett's/Tukey's test).

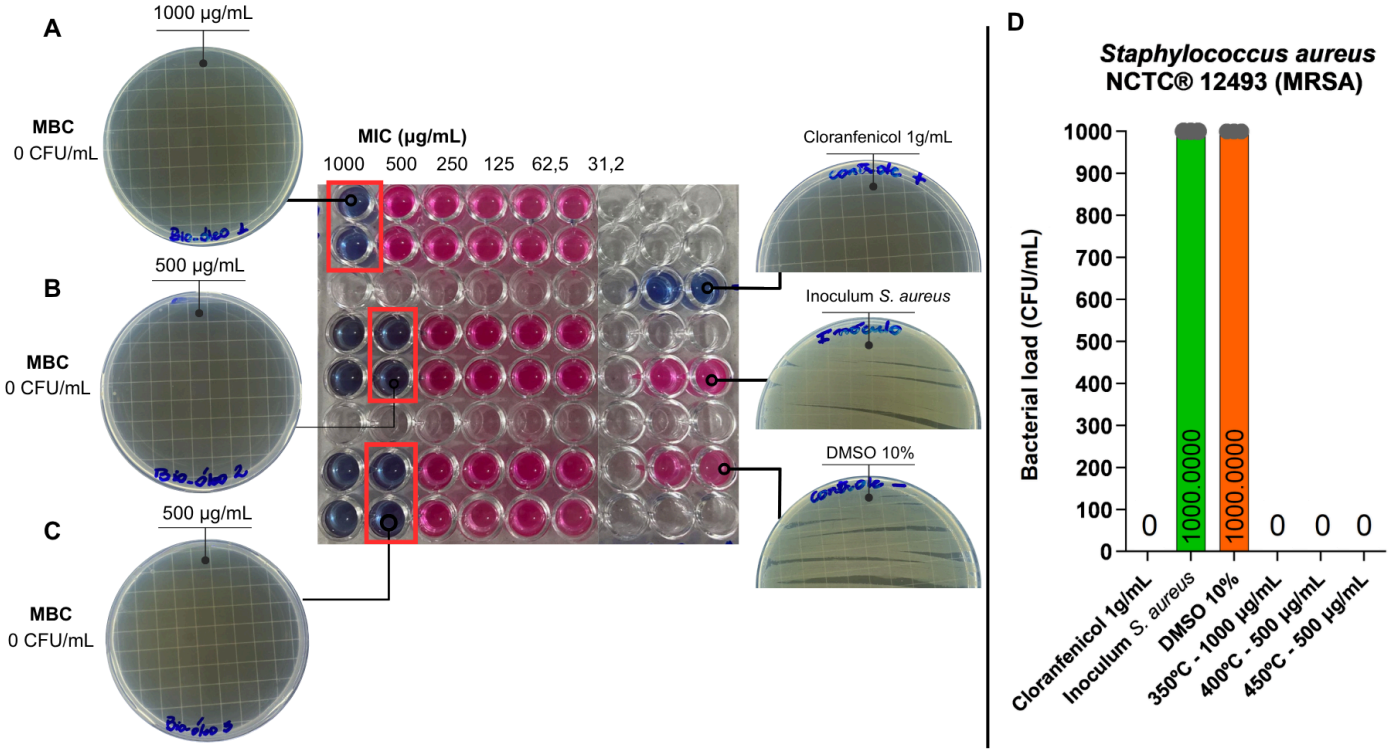


Figure 2

Antibacterial activity of açaí seed bio-oils against MRSA NCTC 12493. Resazurin broth microdilution plate showing the MIC (red boxes) and the corresponding MBC plates for the bio-oils produced at 350 °C (A; 1000 µg/mL), 400 °C (B; 500 µg/mL) and 450 °C (C; 500 µg/mL). Blue wells indicate no growth and pink wells indicate bacterial growth. Controls: chloramphenicol (positive control), untreated inoculum (growth control) and 10% DMSO (vehicle control). (D) Colony counts recovered from the MIC wells and controls, shown as median and IQR (Kruskal–Wallis test followed by Dunn's test; comparisons with p > 0.05 vs. the positive control are not shown).

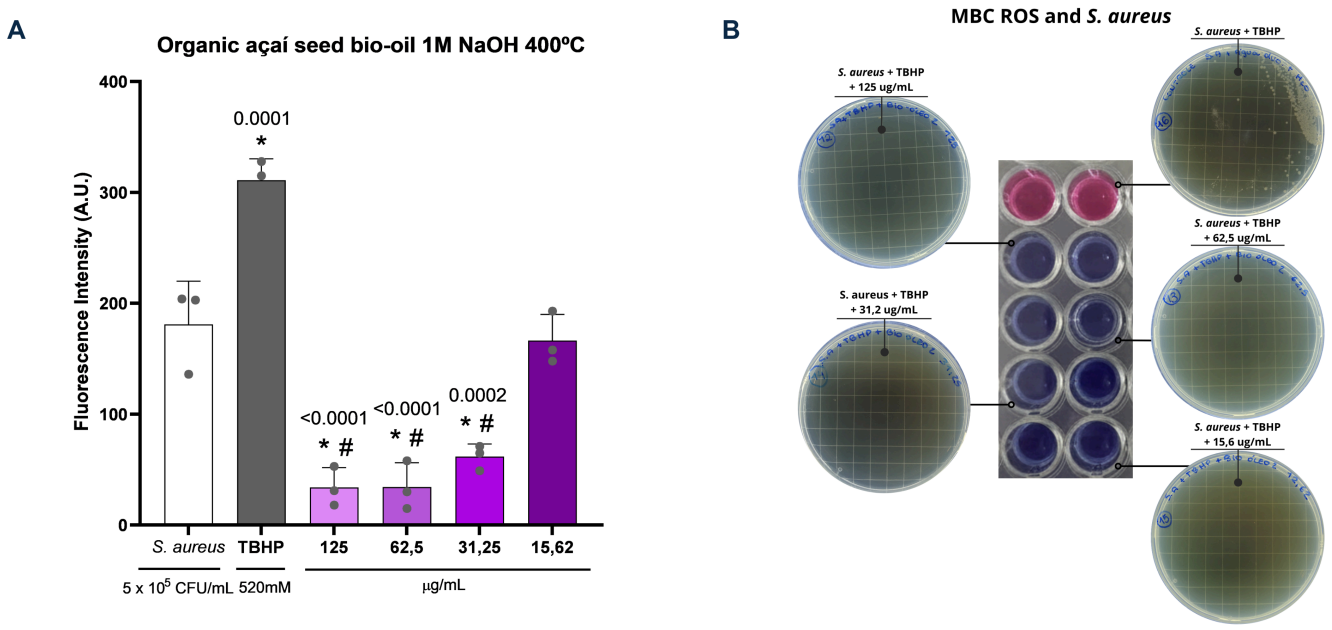


Figure 3

Effect of the 400 °C açaí seed bio-oil on reactive oxygen species in MRSA. (A) DCF fluorescence (arbitrary units, A.U.) of MRSA NCTC 12493 (5×10^5 CFU/mL) stimulated with TBHP (520 mM) and exposed to the bio-oil (15.62–125 µg/mL). Data are mean ± SD with individual values (one-way ANOVA followed by Tukey's test). *p < 0.05 vs. unstimulated *S. aureus*; #p < 0.0001 vs. TBHP. (B) Bacterial viability at the end of the ROS assay: plates of TBHP-stimulated bacteria exposed to the bio-oil and of the TBHP-only control.

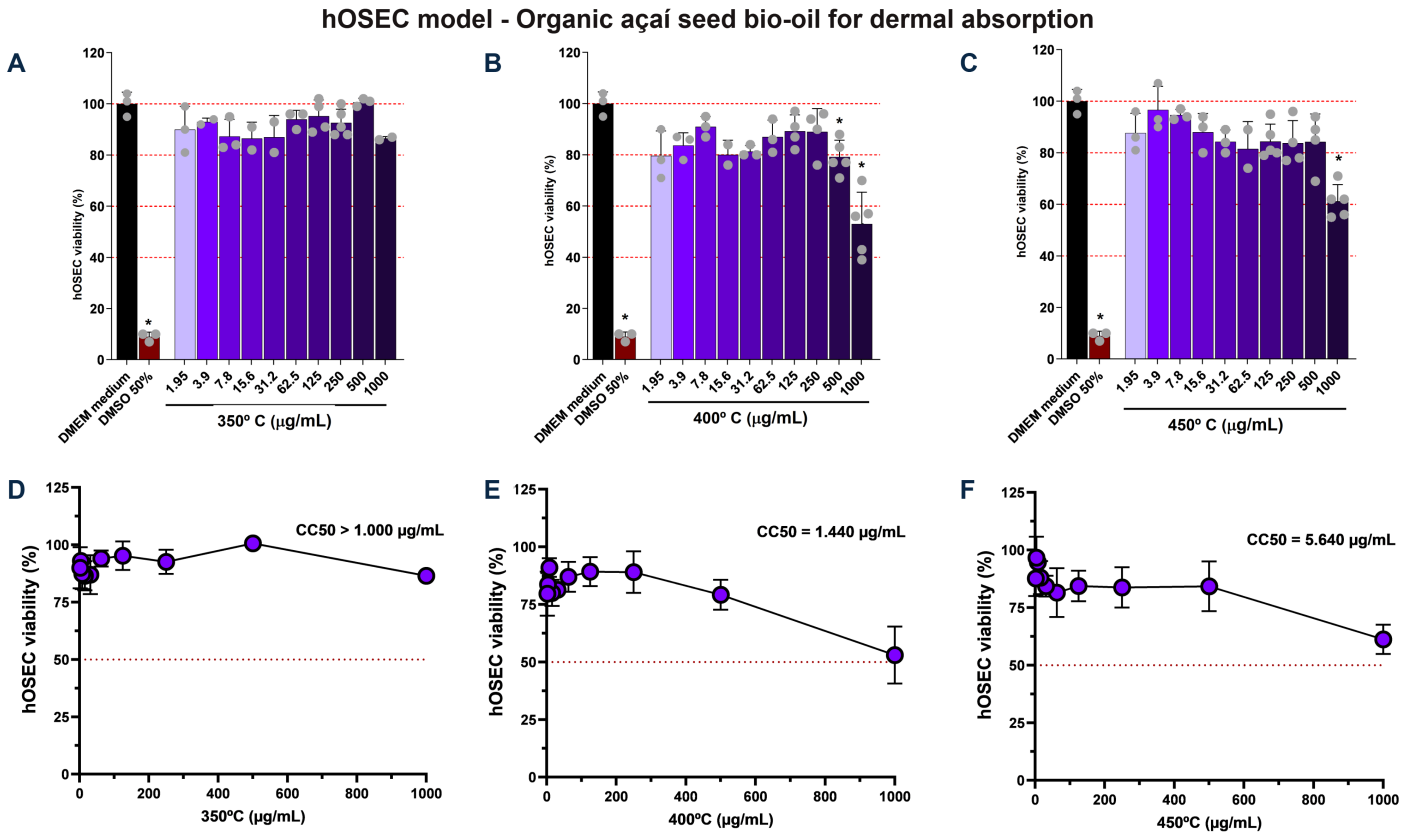


Figure 4

Tissue tolerability of açaí seed bio-oils in the hOSEC model after dermal exposure. Viability of human skin explants exposed for 120 h (medium renewed every 48 h) to bio-oils produced at 350 °C (A, D), 400 °C (B, E) and 450 °C (C, F) (1.95–1000 µg/mL), measured by the TTC assay. (D–F) Concentration–response curves; the dotted line indicates 50% viability. Data are mean ± SD with individual values. *p < 0.05 vs. DMEM (one-way ANOVA followed by Dunnett's/Tukey's test).

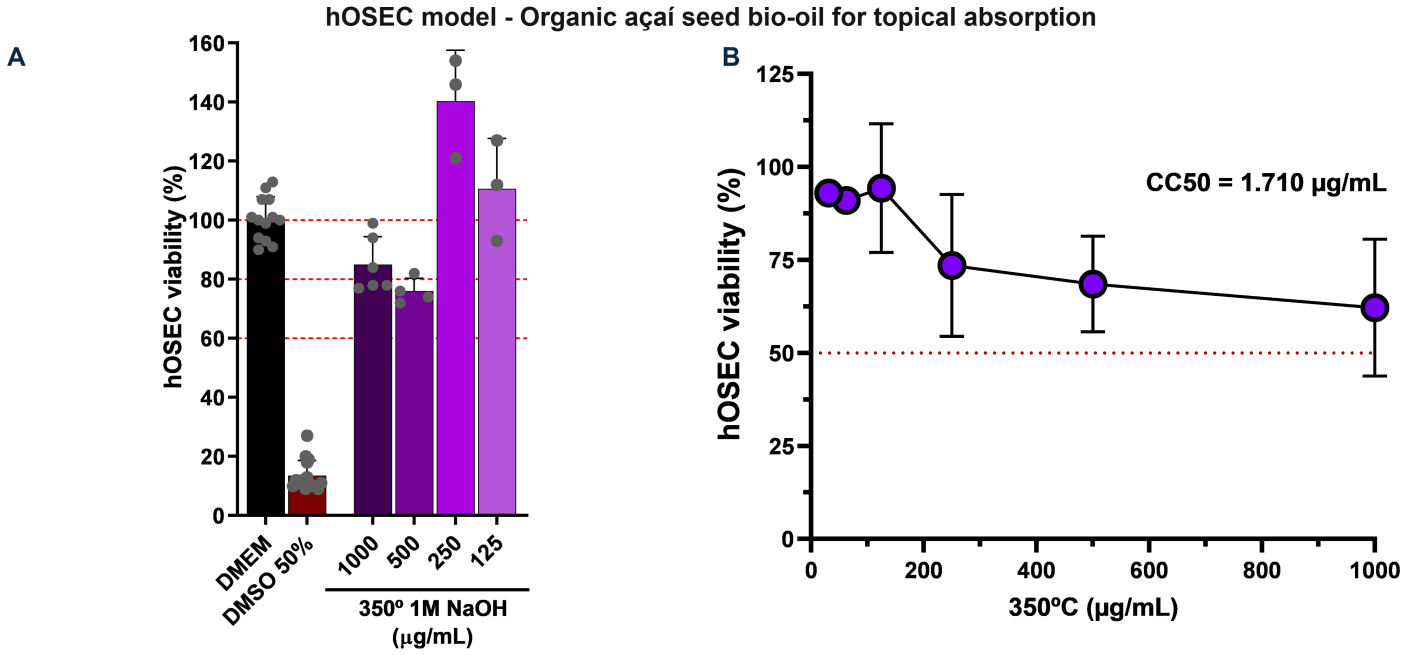


Figure 5

Tissue tolerability of the 350 °C açaí seed bio-oil in the hOSEC model after topical application. (A) Viability of human skin explants after 120 h of topical exposure (125–1000 µg/mL), measured by the TTC assay; data are median and IQR with individual values (Kruskal–Wallis test followed by Dunn's test; no comparison with DMEM reached $p < 0.05$). (B) Concentration–response curve; the dotted line indicates 50% viability.

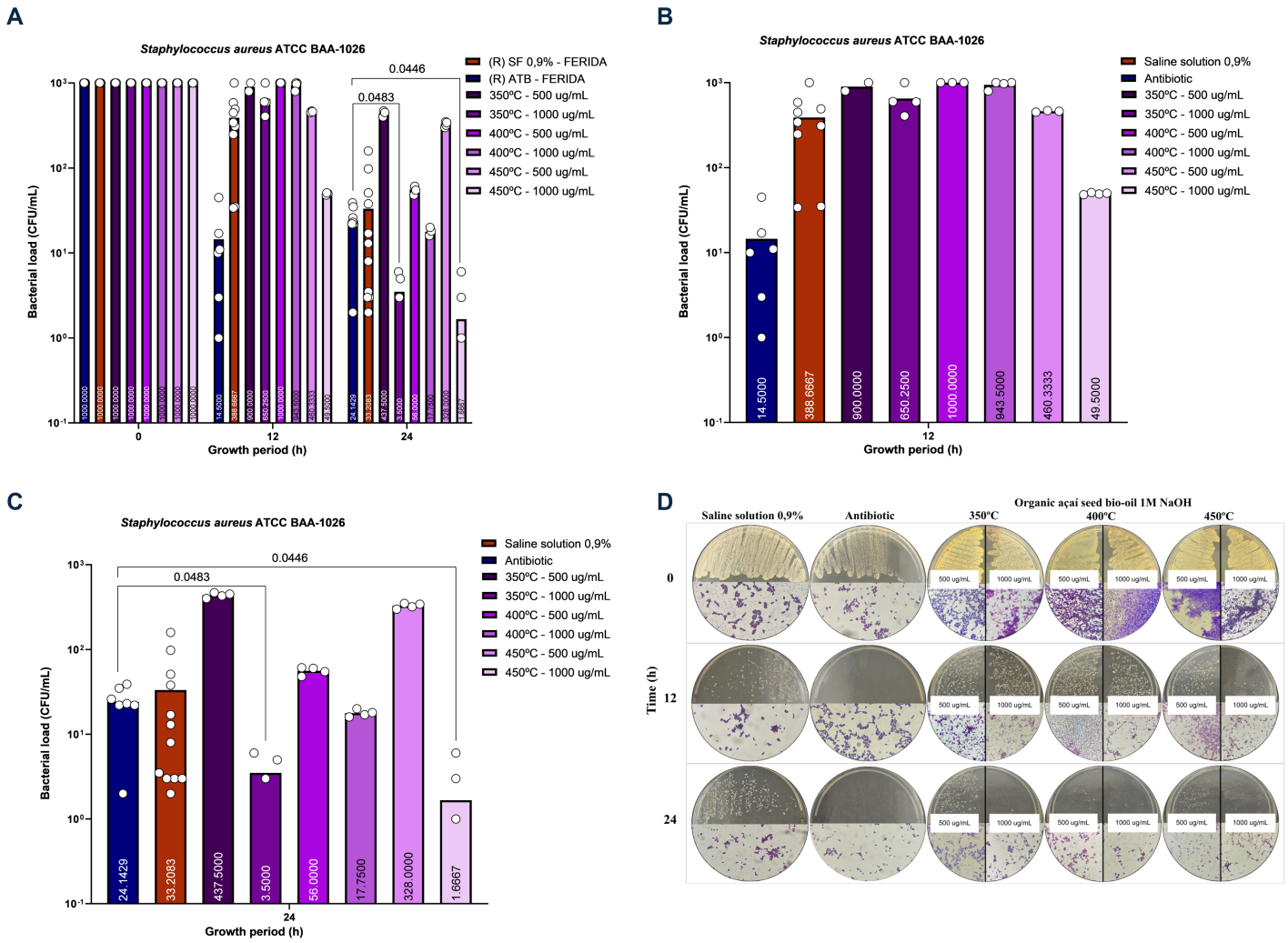


Figure 6

Topical antibacterial activity of açaí seed bio-oils in the wounded hOSEC model. Explants with a 4 mm wound were colonised with *S. aureus* ATCC BAA-1026 for 24 h and treated once with 0.9% saline, antibiotic–antimycotic solution or bio-oils produced at 350, 400 and 450 °C (500 and 1000 µg/mL). Bacterial counts at 0 h (A), 12 h (B) and 24 h (C) after treatment; explants from three donors processed in triplicate; bars indicate median and points individual values (Kruskal–Wallis test followed by Dunn's test; p values vs. antibiotic are shown). (D) Representative culture plates (upper half) and Gram-stained smears (lower half) of each group at 0, 12 and 24 h.

Supplementary Files

This is a list of supplementary files associated with this preprint. Click to download.

- Graphicalabstract.png